Journal of Neuroscience Methods 136 (2004) 197–205

JOURNAL OF NEUROSCIENCE METHODS

www.elsevier.com/locate/jneumeth

Optimising coherence estimation to assess the functional correlation of tremor-related activity between the subthalamic nucleus and the forearm muscles

Shou-Yan Wang [a,b], Xuguang Liu [a,c,*], John Yianni [b], R. Christopher Miall [a], Tipu Z. Aziz [a,b,c], John F. Stein [a]

[a] *University Laboratory of Physiology, University of Oxford, Oxford OX1 3PT, UK*
[b] *The Movement Disorder Group, Department of Neurological Surgery, Radcliffe Infirmary, Oxford OX2 6HE, UK*
[c] *The Movement Disorders and Neurostimulation Group, Department of Neurosciences, 12 East, Charing Cross Hospital, London W6 8RF, UK*

Received 6 October 2003; received in revised form 16 January 2004; accepted 19 January 2004

Abstract

Application of coherence estimation needs not only to correctly estimate coherence values but also to efficiently test the statistical significance of the estimates. In the present report, we have explained the approach of optimising a coherence estimator by restricting its normalised bias error and random error. In addition to the commonly used independence threshold, two more tests based on the probability of detection and the exact confidence interval have been proposed for detecting the significance of the coherence estimates. All three methods have been used to evaluate the significant functional correlation between oscillatory field potentials (FPs) in the subthalamic nucleus (STN) and the surface electromyogram (EMG) of the forearm muscles during tremor in Parkinson's disease.
© 2004 Elsevier B.V. All rights reserved.

Keywords: Coherence estimation; Statistics; Field potential; Subthalamic nucleus; Electromyogram; Parkinson's disease; Tremor

1. Introduction

One widely used method of estimating the functional coupling between two oscillatory signals is the magnitude squared coherence (MSC) estimation. The MSC is a normalized cross-spectral density function, and measures the strength of association and relative linearity between two stationary processes on a scale from 0 to 1 (Bendat and Piersol, 1993; Brillinger, 1975; Carter, 1987; Halliday et al., 1995). In order to test the significance of the coherence and use it in practical applications properly, it is highly desirable to compute the statistics of the estimator exactly. The exact and asymptotic expressions have been deduced for the probability density function, cumulative distribution function, and for the bias and variance (Brillinger, 1975; Carter, 1987; Carter et al., 1973; Clausen and Cochran, 2001). However, a significant limitation encountered in application of the MSC estimate is that only in some particular conditions, for example when coherence is 0 or 1, it is possible to provide the closed-form expression for the confidence interval. In other situations, the confidence interval is only given approximately (Bendat and Piersol, 1993, 2000; Brillinger, 1975; Carter, 1987; Carter et al., 1973). Consequently, the distribution range of coherence estimates and the comparison between different coherence estimates are questionable, especially when the amount of data is relatively limited. Furthermore, to avoid inadequate and inaccurate estimation, the performance of an estimator and its validation on the data to be analysed needs to be evaluated, and the estimation may require multiple statistical tests. In this study, we validated the estimation by limiting the normalised bias error and the random error. In addition to the existing statistical test for independence between two signals, two extra statistical tests are proposed: (1) to measure the probability of detection of the MSC estimates to confirm the existence of significant linear association; and (2) to apply the exact confidence intervals based on the cumulative distribution

Abbreviations: STN, subthalamic nucleus; FPs, field potentials; DBS, deep brain stimulation; EMGs, electromyograms; MSC, magnitude squared coherence

* Corresponding author. Tel.: +44-20-88467631; fax: +44-20-88467487.
E-mail address: x.liu@ic.ac.uk (X. Liu).

0165-0270/$ – see front matter © 2004 Elsevier B.V. All rights reserved.
doi:10.1016/j.jneumeth.2004.01.008

function, which can be used to determine the significance of the estimation differing from 0 and the significance of the differences of components at different frequencies.

Oscillatory neural activity in deep brain structures has attracted much interest in both clinical practice and research on movement disorders and other neurological conditions (Brown et al., 1999; Liu et al., 2001, 2002a,b; Marsden et al., 2000). Although there are still uncertainties about the precise function and genesis of the oscillations, analysis of functional coupling between simultaneously recorded oscillations at different levels of the motor system has provided important information. It has led not only to a better understanding of the pathophysiological mechanisms of movement disorders but also to better localization of targets for deep brain stimulation (DBS). However, these symptom-related muscular and neuronal signals are only stationary over a short period, are contaminated with noise, and their coherence is relatively weak. These features of the real physiological signals present particular technical challenges for investigating the functional correlation between simultaneously recorded neuronal and muscular signals.

Hence, in this report, we propose algorithms for optimising a coherence estimator and generating supplementary statistical tests. We present an example of applying these procedures in assessing the functional correlation between tremor-related oscillatory field potentials (FPs) and the electromyogram (EMG) in patients with Parkinson's disease.

2. Methods

2.1. Magnitude squared coherence estimation

The MSC function between two jointly stationary stochastic processes $x(t)$ and $y(t)$ is defined by:

$$\gamma_{xy}^2(f) = \frac{|P_{xy}(f)|^2}{P_{xx}(f)P_{yy}(f)} \tag{1}$$

where $P_{xy}(f)$ is the complex cross-spectral density, and $P_{xx}(f)$ and $P_{yy}(f)$ are the auto-spectral densities at frequency f (Bendat and Piersol, 1993, 2000; Brillinger, 1975; Carter, 1987; Halliday et al., 1995).

MSC can be estimated using the weighted overlapped-segment averaging method based on fast Fourier transform. In this method, two signals are divided into n_d disjoint segments; each segment is multiplied by a smooth weighting window, and then the averaged cross-spectra density and the auto-spectral densities are obtained from the n_d segments. MSC is the normalized cross-spectral density by the auto-spectral densities.

$$\hat{\gamma}_{xy}^2(f) = \frac{\left|\sum_{i=1}^{n_d} X_i(f)Y_i^*(f)\right|^2}{\sum_{i=1}^{n_d}|X_i(f)|^2 \sum_{i=1}^{n_d}|Y_i(f)|^2} \tag{2}$$

Here, * denotes the complex conjugate, $X_i(f)$ and $Y_i(f)$ are the fast Fourier transform (FFT) of the ith of the weighted segments of the stochastic processes $x(t)$ and $y(t)$ (Bendat and Piersol, 1993; Brillinger, 1975; Carter, 1987; Carter et al., 1973). The stochastic processes are assumed to be 0 mean, jointly stationary Gaussian stochastic processes. To obtain a reliable estimator, some assumptions are necessary (Halliday et al., 1995; Scannell and Carter, 1978). They are that: (a) the data segments are independent, (b) the data segments are multiplied by a smooth weighting window to reduce sidelobe leakage, (c) each data segment is sufficiently long to ensure adequate spectral frequency resolution and reduce the bias, and (d) the number of the data segments is sufficient to make the estimator achieve reliable statistic performance.

2.2. Optimisation of a coherence estimator

2.2.1. Probability density function, cumulative distribution function, bias error and random error

Given the true value of coherence γ_{xy}^2 and the number of non-overlapped data segments n_d, the probability density function and the cumulative distribution function of the estimator are (Carter, 1987):

$$p(\hat{\gamma}_{xy}^2|n_d, \gamma_{xy}^2) = (n_d - 1)\left(\frac{(1-\hat{\gamma}_{xy}^2)(1-\gamma_{xy}^2)}{(1-\hat{\gamma}_{xy}^2\gamma_{xy}^2)^2}\right)^{n_d} \times \left(\frac{1-\hat{\gamma}_{xy}^2\gamma_{xy}^2}{(1-\hat{\gamma}_{xy}^2)^2}\right) {}_2F_1(1-n_d, 1-n_d; 1; \hat{\gamma}_{xy}^2\gamma_{xy}^2) \tag{3}$$

$$P(\hat{\gamma}_{xy}^2|n_d, \gamma_{xy}^2) = \hat{\gamma}_{xy}^2\left(\frac{1-\gamma_{xy}^2}{1-\hat{\gamma}_{xy}^2\gamma_{xy}^2}\right)^{n_d} \sum_{k=0}^{n_d-2} \times \left(\frac{1-\hat{\gamma}_{xy}^2}{1-\hat{\gamma}_{xy}^2\gamma_{xy}^2}\right)^k {}_2F_1(-k, 1-n_d; 1; \hat{\gamma}_{xy}^2\gamma_{xy}^2) \tag{4}$$

The hypergeometric function ${}_2F_1$ can be computed iteratively when γ_{xy}^2 is not equal to 0 (Carter, 1977, 1987).

$${}_2F_1(-k, 1-n_d; 1; \hat{\gamma}_{xy}^2\gamma_{xy}^2) = \sum_{i=0}^{k} T_i \tag{5}$$

where $T_0 = 1$ and

$$\frac{T_i}{T_{i-1}} = \frac{(i-1-k)(i-n_d)\hat{\gamma}_{xy}^2\gamma_{xy}^2}{i^2}$$

The exact expression of the bias and variance (Carter, 1987) are:

$$B = \frac{1}{n_d} + \frac{n_d - 1}{n_d + 1}\gamma_{xy}^2 {}_2F_1(1, 1; n_d + 2; \gamma_{xy}^2) - \gamma_{xy}^2 \tag{6}$$

$$V = \frac{2(1-\gamma_{xy}^2)^{n_d}}{n_d(n_d+1)} {}_3F_2(3, n_d, n_d; n_d + 2, 1; \gamma_{xy}^2) - \left[\frac{(1-\gamma_{xy}^2)^{n_d}}{n_d} {}_3F_2(2, n_d, n_d; n_d + 1, 1; \gamma_{xy}^2)\right]^2 \tag{7}$$

where ${}_3F_2$ is a five parameter Gaussian hypergeometric function. The greatest bias is $1/n_d$ when the MSC equals 0 and greatest variance is $(2/3)^3/n_d$ when the MSC equals one third. The ratio of bias and γ_{xy}^2 is the normalized bias error ε_b and the ratio of variance and γ_{xy}^2 is the random error ε_r.

2.3. Exact confidence interval of coherence estimates

The confidence interval of the coherence estimates can be derived from the central probability interval of the cumulative distribution function (Carter, 1987; Stuart et al., 1999, 2001). Given a true coherence value γ_{xy}^2, there is a central probability interval $[A_L(\gamma_{xy}^2), A_U(\gamma_{xy}^2)]$ which meets the following conditions,

$$P(\hat{\gamma}_{xy}^2 \le A_L(\gamma_{xy}^2)|n_d, \gamma_{xy}^2) = \alpha_0 \tag{8a}$$

$$P(\hat{\gamma}_{xy}^2 \le A_U(\gamma_{xy}^2)|n_d, \gamma_{xy}^2) = 1 - \alpha_0 \tag{8b}$$

Then $P(A_L(\gamma_{xy}^2) \le \hat{\gamma}_{xy}^2 \le A_U(\gamma_{xy}^2)|n_d, \gamma_{xy}^2) = 1 - 2\alpha_0$. It is a reasonable assumption that $A_L(\gamma_{xy}^2)$ and $A_U(\gamma_{xy}^2)$ are monotonically increasing with γ_{xy}^2 and are continuous (Carter, 1987). Then we have,

$$\Pr(A_U^{-1}(\hat{\gamma}_{xy}^2) \le \gamma_{xy}^2 \le A_L^{-1}(\hat{\gamma}_{xy}^2)|n_d, \gamma_{xy}^2) = 1 - 2\alpha_0 \tag{9}$$

Therefore, the confidence interval for $\hat{\gamma}_{xy}^2$ is $[A_U^{-1}(\hat{\gamma}_{xy}^2), A_L^{-1}(\hat{\gamma}_{xy}^2)]$ with confidence coefficient $1 - 2\alpha_0$.

Usually the functions $A_L(\gamma_{xy}^2)$, $A_U(\gamma_{xy}^2)$, $A_U^{-1}(\hat{\gamma}_{xy}^2)$ and $A_L^{-1}(\hat{\gamma}_{xy}^2)$ are unknown. We provided an iterative algorithm to obtain the solution (more details on the iterative algorithm can be found in Wang and Tang, 2004). Given the number of disjoint segments n_d and the true coherence values γ_{xy}^2, the cumulative distribution function corresponding to $\hat{\gamma}_{xy}^2$ can be computed as described above (4) (Fig. 2(a)). Therefore, the value of $\hat{\gamma}_{xy}^2$ is $A_L(\gamma_{xy}^2)$ or $A_U(\gamma_{xy}^2)$ while the value of cumulative distribution function equals lower or upper probability limit. The lower and upper probability limits are 0.05 and 0.95 in order to estimate the confidence intervals with 0.90 confidence coefficient (Fig. 2(a)). $A_L(\gamma_{xy}^2)$ or $A_U(\gamma_{xy}^2)$ can be obtained when the cumulative distribution function approaches to the lower or upper probability with $\hat{\gamma}_{xy}^2$ modified iteratively (Fig. 2(b)).

After $\gamma_{xy}^2(i) \sim A_L(\gamma_{xy}^2(i))$ and $\gamma_{xy}^2(i) \sim A_U(\gamma_{xy}^2(i))$ curves are computed using above iterative algorithm, $\hat{\gamma}_{xy}^2(i) \sim A_U^{-1}(\hat{\gamma}_{xy}^2(i))$ and $\hat{\gamma}_{xy}^2(i) \sim A_L^{-1}(\hat{\gamma}_{xy}^2(i))$ can be obtained by reflecting the curves across the line $\gamma_{xy}^2 = A_L(\gamma_{xy}^2)$ or $\gamma_{xy}^2 = A_U(\gamma_{xy}^2)$.

2.4. Statistical tests for the significance of independence and coherence

One way of determining the significance of the estimated coherence is based on the confidence interval of the estimates. Given the true value of coherence γ_{xy}^2 and the number of disjointed data segments n_d, the exact forms of the conditional probability density function $p(\hat{\gamma}_{xy}^2|n_d, \gamma_{xy}^2)$ and the cumulative distribution function $P(\hat{\gamma}_{xy}^2|n_d, \gamma_{xy}^2)$ of the estimator can be obtained from (3) and (4). From the probability density function, a threshold E_I is defined to test the independence at a given probability P_I (10). The hypothesis of MSC = 0 at each frequency value rather than the whole spectrum is then tested against the independence threshold E_I (11) (Brillinger, 1975; Carter, 1987; Halliday et al., 1995; Zaveri et al., 1999). Coherence estimates below this threshold suggests that the two processes are independent.

$$P_I = \int_0^{E_I} p(\hat{\gamma}|n_d, 0)d\hat{\gamma} = \int_0^{E_I} (n_d - 1)(1 - \hat{\gamma})^{(n_d-2)}d\hat{\gamma} \tag{10}$$

$$E_I = 1 - (1 - P_I)^{1/(n_d-1)} \tag{11}$$

We set the level of significance $\alpha = 0.05$, then the confidence interval for $\gamma_{xy}^2 = 0$ is $[0, E_I]$ with confidence coefficient 0.95 and P_I is 0.95. The one side confidence interval for $\hat{\gamma}_{xy}^2$ is $[A_U^{-1}(\hat{\gamma}_{xy}^2), 1]$ with confidence coefficient 0.95. Here $A_U^{-1}(\hat{\gamma}_{xy}^2)$ equals the lower confidence limit of the both sides confidence interval with confidence coefficient 0.90, which can be computed using the method described in 2.2. The hypothesis H_0: MSC > 0 against H_1: MSC = 0 is tested by the comparison of the confidence intervals. If $A_U^{-1}(\hat{\gamma}_{xy}^2) > E_I$, H_0 is accepted with $\alpha < 0.05$, the MSC is larger than 0 significantly and there is true coherence between the two processes.

Another way to determine the significance of the coherence estimate is based on the probability of detection. Coherence estimates below the independence threshold suggest that the two signals being analysed are independent. On the other hand, the coherence estimates above the threshold E_I can be seen as the evidence of linear association between two processes at a certain probability of detection P_D (11) (Carter, 1987; Zaveri et al., 1999), and the probability of detection P_D is computed as

$$P_D = \int_{E_I}^1 p(\hat{\gamma}|n_d, \gamma_{xy}^2)d\hat{\gamma} = 1 - P(\hat{\gamma} \le E_I|n_d, \gamma_{xy}^2) \tag{12}$$

The true coherence γ_{xy}^2 is unknown in most situations. For practical application, one way is to replace γ_{xy}^2 with the estimated coherence $\hat{\gamma}_{xy}^2$ while the number of the data segments n_d is large and $\hat{\gamma}_{xy}^2$ is great enough.

3. EMG and LFPs recording

Local field potentials (LFPs) were recorded from the subthalamic nucleus (STN) in three patients after implantation of chronic stimulation electrodes for alleviating their Parkinsonian symptoms at Radcliffe Infirmary, Oxford. Informed consent from the patients and the approval of the local ethics committee were obtained for this research. Detailed

surgical and neurophysiological procedures have been described previously (Liu et al., 2001, 2002b). The LFPs were recorded via the implanted electrode (DBS™, models 3387 Medtronic®). All signals were filtered with bandwidth of 0.5–1000 Hz, sampled at 4000 Hz, amplified at 1000× (CED 1902, Cambridge Electronic Design, UK) and digitized with 16-bit resolution (CED 1401, Cambridge Electronic Design, UK). Surface EMGs from the contralateral forearm extensor (*carpi ulnaris*) and flexor (*digitorum profundus*) were simultaneously recorded while the patients were sitting. The EMGs were filtered between 31 and 2000 Hz to reduce the sustained activity imposed on the rhythmic tremor activity using discrete wavelet transform.

4. Computing

Computation of the cumulative distribution functions, exact confidence intervals, relationship between the n_d value and coherence at the given normalized bias error and random error, the probability of detection and coherence estimation between STN FPs and EMGs was performed using MATLAB (Version 5, MathWorks Inc., Natick, MA, USA). The coherence was estimated using 150 s data with 15 or 2 s non-overlapping windows, which gives a value of $n_d = 10$ or 75.

5. Results

Four levels of the normalized bias error curves and three levels random error curves are illustrated in Fig. 1. While the coherence increases, in order to keep the normalized bias error or the random error at the specified level, the necessary minimum number of data segments decreases gradually. However, while the coherence approaches 0, the necessary number increases dramatically. If the coherence is 0.3, the necessary number to keep the normalised bias error = 0.1 is 17 while 81 data segments are needed to keep the random error = 0.2. The number of segments needed increases to 181 and 908, respectively, if the coherence is 0.05. The shadow areas indicate the normalized bias error below 0.1 (Fig. 1(a)) and the random error below 0.2 (Fig. 1(b)). So the bias error and random error of the data can be determined from Fig. 1. If the coherence is likely to be low, the number of data segments must be high enough to keep the random error and bias error within an acceptable level. Hence, one can estimate the n_d required to ensure a particular level of coherence estimates credible with acceptable error.

The cumulative distribution functions of $\hat{\gamma}^2_{xy}$ for $\gamma^2_{xy} =$ 0.05, 0.5 and 0.9 and $n_d = 10$ are illustrated in Fig. 2(a). When the cumulative distribution functions equal to the upper or lower probability limits 0.95 or 0.05, the corresponding values of $\hat{\gamma}^2_{xy}$ which are computed using the iterative algorithm, are used to construct the central probability interval $\gamma^2_{xy}(i) \sim A_U(\gamma^2_{xy}(i))$ or $\gamma^2_{xy}(i) \sim A_L(\gamma^2_{xy}(i))$ (Fig. 2(b)). Then the confidence interval with confidence coefficient 0.9

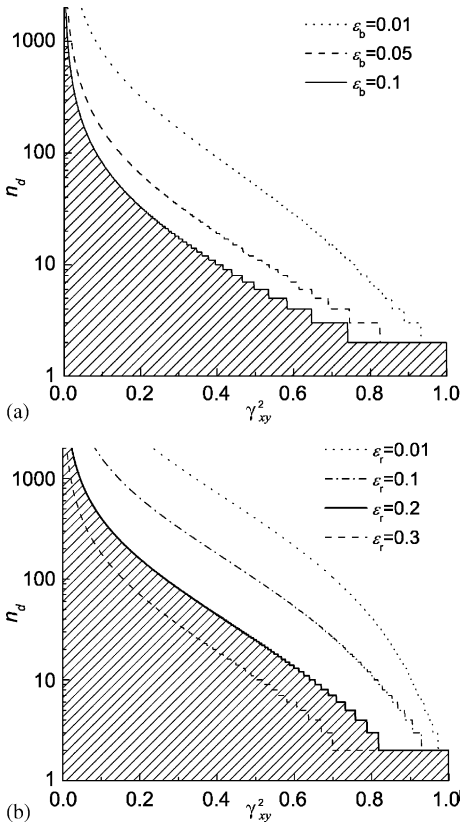

Fig. 1. Relationship between the n_d value and coherence at the given normalised bias error and random error. (a) The normalized bias error ε_b at levels of 0.1, 0.05 and 0.01. The shadow area indicates the normalized bias error larger than 0.1. (b) The random error ε_r at levels of 0.3, 0.2, 0.1 and 0.01. The shadow area indicates the random error larger than 0.2. When estimated MSC is weak with a small value, a large n_d value is required to assure the bias and random error being kept at an acceptable level.

$\hat{\gamma}^2_{xy}(i) \sim A_U^{-1}(\hat{\gamma}^2_{xy}(i))$ and $\hat{\gamma}^2_{xy}(i) \sim A_L^{-1}(\hat{\gamma}^2_{xy}(i))$ are acquired by reflecting the curves across the line $\gamma^2_{xy} = A_L(\gamma^2_{xy})$ or $A_U(\gamma^2_{xy})$.

The exact confidence intervals with confidence coefficient 0.9 for $n_d = 10$, 50, 100 and 200 are drawn in Fig. 3. When the n_d equals 10, the peak value of 95% confidence interval deduced from the cumulative distribution function at the MSC estimate 0.33 is 0.00–0.62. The interval decreases to 0.25–0.40, as the n_d becomes 200. Thus, the 95% confidence interval narrows when n_d increases. The confidence intervals are 0.13–0.27 and 0.32–0.47 for the MSC estimates of 0.20 and 0.40, respectively, when n_d equals 200. There is no overlap between these two confidence intervals; suggesting that there is a significant difference between the MSC estimates of 0.20 and 0.40. While n_d increases, the confidence bound becomes narrower. While the coherence approaches to 0 or 1, the confidence bound becomes 0. The largest confidence bound occurs with coherence at 1/3. The confidence upper and lower limits increase monotonically and continuously.

The detection probability P_D increases with the coherence value. The detection probability is beyond the significant

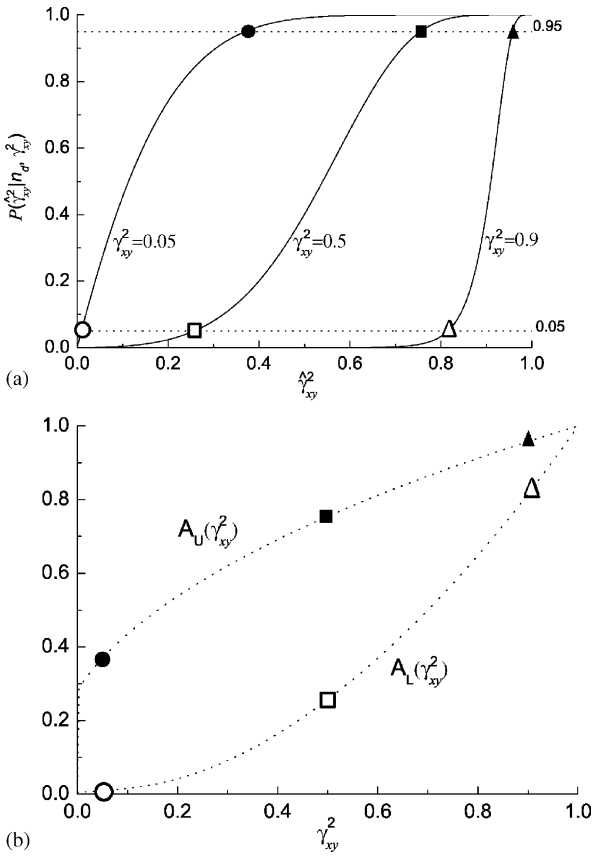

Fig. 2. The cumulative distribution functions of (a) for $\gamma_{xy}^2 = 0.05$, 0.5 and 0.9 and (b) the curves $A_L(\gamma_{xy}^2(i)) \sim \gamma_{xy}^2(i)$ (open symbols) and $A_U(\gamma_{xy}^2(i)) \sim \gamma_{xy}^2(i)$ (solid symbols) derived from the cumulative distribution functions for $\gamma_{xy}^2(i) = 0.05$, 0.5 and 0.9 while $n_d = 10$. The dotted horizontal lines indicate the upper and lower probability limits 0.975 and 0.025.

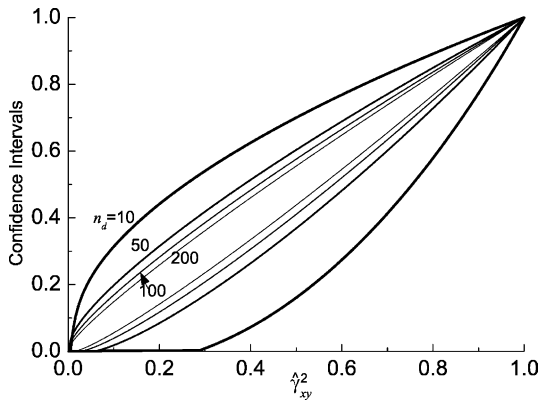

Fig. 3. The exact confidence intervals with 0.90 confidence coefficient when $n_d = 10$, 50, 100 and 200. The pair curves are the upper and lower confidence limits of the coherence estimates. While n_d increases, the confidence bound becomes narrower. While the coherence approaches to 0 or 1, the confidence bound becomes 0. The largest confidence bound occurs with coherence at 1/3. The confidence upper and lower limits increase monotonically and continuously.

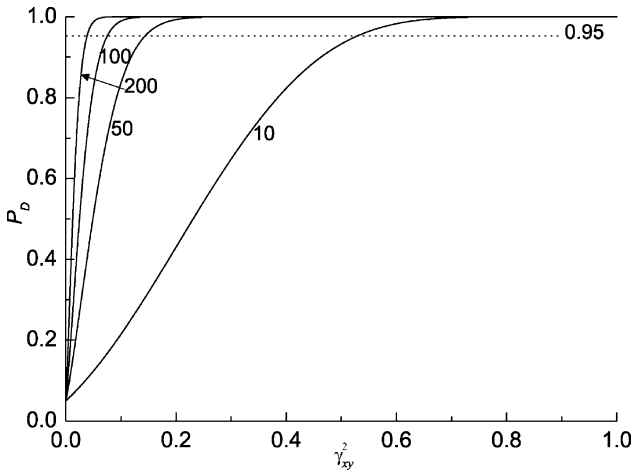

Fig. 4. The probability of detection P_D corresponding to γ_{xy}^2 with $n_d = 10$, 50, 100, and 200. The linear association between the random processes can be announced at the probability of detection P_D corresponding to a MSC value. To reach a significant probability of detection, a large n_d is required for detecting small MSC values. The dotted line indicates the significant probability of 0.95.

level 0.95 when the coherence is larger than a threshold value (Fig. 4). This threshold value decreases while n_d increases. For n_d 10, the independence threshold E_I is 0.283, but γ_{xy}^2 is 0.525 while the detection probability equals to 0.95. However, for n_d 200, the independence threshold E_I is 0.015, γ_{xy}^2 only reaches as small as 0.038 while P_D equals to 0.95 (Table 1). Furthermore, the detection probability P'_D is estimated using the biased coherence value $\gamma_{xy}^2 + B$. For n_d 10, 50, 100 and 200, P'_D equals near to 0.97 while the true detection probability is 0.95 (Table 1). The small

Table 1
The detection probability P_D computed from the true coherence γ_{xy}^2 and P'_D computed from the biased coherence $\gamma_{xy}^2 + B$ while they are above the independence threshold E_I

γ_{xy}^2	P_D	P'_D	P_D	P'_D	P_D	P'_D	P_D	P'_D
0.038	–	–	–	–	0.698	0.800	0.95	0.969
0.074	–	–	0.697	0.796	0.95	0.969	0.999	1
0.142	–	–	0.95	0.969	0.999	1	1	1
0.525	0.95	0.964	1	1	1	1	1	1
n_d	10		50		100		200	
E_I	0.283		0.059		0.030		0.015	

B is the bias of the estimator; n_d, number of disjoint data segments. The biased probability of detection is near to 0.97 while the true value is 0.95.

significant coherence can be detected while the number of data segments is large.

As an example of applying these method to physiological data, the coherence estimation between flexor EMG and the STN FPs recorded from a Parkinsonian patient during tremor was performed over windows of 15 or 2 s in length. These window lengths gave the frequency resolution of 0.067 or 0.5 Hz for presenting the coherence in the tremor frequency. The overall length of the signal analysed was 150 s, which provided 10 or 75 non-overlapped windows. The results showed that there were two dominant peaks beyond the independence threshold in the coherence estimates in the frequency range of 0−20 Hz. With 10 non-overlapped windows, the peak coherence value at 4.8 Hz was 0.74, where the detection probability was 0.98 and the lower bound of the 90% confidence interval [0.47, 0.85] was beyond the independence threshold 0.28. However, at 9.4 Hz the peak coherence value was 0.50, the detection probability was below 0.95 and the lower bound of the 90% confidence interval was below the independence threshold. In comparison with the estimation with 75 non-overlapped windows, the peak coherence value at 4.7 Hz was 0.26, but the detection probability was close 1.0 and the lower bounds of the 90% confidence interval 0.15 and 0.12 were well above the independence threshold 0.04 at 4.7 and 9.5 Hz. Furthermore, the phase values were more stable in estimation with 75 windows than that with 10 windows.

6. Discussion

In the present report, we have attempted to enhance the efficiency of the coherence estimation. We proposed the guidance for validating the reliability of the significant coherence estimates based on their normalized bias error and random error. Two more statistical tests based on the exact confidence interval and the detection probability are proposed for testing significance of coherence estimates.

We evaluate the estimator performance by calculating the errors of the estimates because the estimates of MSC are random variables. The performance of an estimator is usefully characterised by the random error and bias error, thus the performance can be improved by minimizing the random error and bias error. In the most commonly employed weighted overlapped-segment averaging coherence estimator, two signals with overall length P can be divided into a number of segments in certain length (T). n_d means the segments are disjointed or zero-overlap between segments; whereas n_o implies data segments are overlapped over certain length (L). Coherence is estimated by averaging the cross-spectra normalized with auto-spectra from n_o signal segments. The performance of an estimator is influenced mainly by three parameters: (1) segment length T, (2) number of the data segments n_d, and (3) overlap fraction L.

The segment length T should be large enough to cover the entire cycle of the dominant component in the signals and to avoid the bias error from the bulk time delay between the signals. In addition, the frequency resolution of coherence estimation based on the Fourier transform is inversely proportional to the segment length T, thus T should be large enough to provide adequate spectral resolution for differentiating components of the signals. Besides the bias from the limited signal length, there is another type of bias due to rapidly changing phase (Carter, 1987). If the phase angle of the cross-power spectrum varies rapidly as a function of frequency, the estimated coherence can be biased. The downward bias approximately equals to $(|D|^2/T^2 - 2|D|/T)\gamma_{xy}^2$ or $-(2|D|/T)\gamma_{xy}^2$ while $|D|$ is much smaller than the length of each data segment T. Here, D is the group delay computed as the slope of the phase and its unit is seconds. To practically reduce this type of bias, one can set a larger size for each data segment or realign the two signals to compensate for the time delay between them. When the phase is relatively stable over the frequency range of interest, for instance at 4.8 and 9.7 Hz in Fig. 5(c), the bias due to rapidly changing phase is negligible.

In the case of zero-overlap, given the overall length of the signals P, the number of data segments n_d is inversely related to the segment length T. From (3) and (4) n_d is shown as an influential parameter of the probability distribution of the estimates and thus affects its bias and variance. Therefore, an adequate number of disjoint data segments must be selected based on an acceptable level of bias and random errors. We have proposed a practical guide for selecting a reliable value of n_d based on the normalized bias error and random error of estimation with a certain MSC value. In practice, the maximum acceptable normalized bias error was thought as 0.1 and less than 0.05 will be ideal (Bendat and Piersol, 1993). For an estimated coherence value with an n_d, one can validate the estimation based on the normalized bias error curves (Fig. 1(a)). If the cross-point of the coherence value and n_d value falls into the shadowed area, the bias error is larger than 0.1, suggesting a larger number of segments is needed for smaller coherence values. Similarly, the random error is larger than the maximal acceptable value of 0.2 (Bendat and Piersol, 1993) if the cross-point of the coherence value and n_d value falls into the shadowed area in Fig. 1(b). Estimator performance will be improved as increase in value n_d and decrease in bias and random errors. For the same value of n_d, on the other hand, the higher value of the true MSC is, the less bias and random errors.

The performance of the estimator can also be improved by the overlapped-segment averaging which makes more efficient use of the data when forming the MSC estimate. The bias and random errors could be reduced further by overlapping the data although at the increased computational costs. Twenty-five to fifty percent overlap is quite reasonable in practice (Carter, 1987; Kay, 1987). However, while the overlap increases from 60 to 90%, the bias and variance decrease slightly but the computation load increases dramatically.

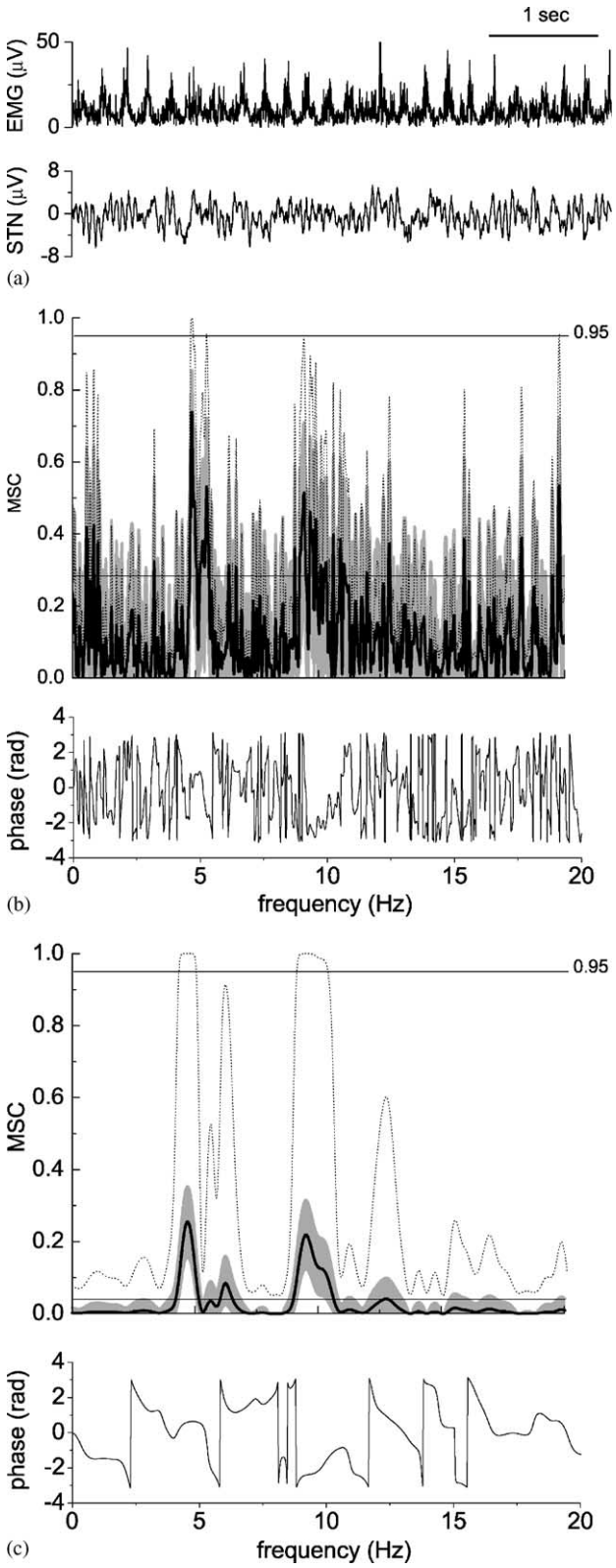

Fig. 5. Coherence estimation between STN PFs and EMGs during tremor. (a) The rectified flexor EMGs and STN LFPs. Coherence estimation (thick solid line) between EMGs and LFPs with non-overlap windows of 15 s (b) and 2 s, superimposed with three different statistic tests. Dotted line: The probability of detection; grey area: the exact confidence interval of 90%; upper horizontal line: 95% probability of detection; and lower horizontal line: the independence threshold.

When the coherence estimation is used to measure the association and linearity between two stationary stochastic processes, it is necessary to specify an interval with certain confidence that the true coherence falls in. Some types of approximate confidence intervals were given in previous works (Bendat and Piersol, 1993, 2000; Brillinger, 1975; Scannell and Carter, 1978). The approximate confidence intervals are reliable under the assumption that the random error is small and data are sufficient (Bendat and Piersol, 1993, 2000). But in many circumstances the signals, especially biomedical signals, are stationary only in short duration, and the coherence is usually weak. Hence knowing the exact confidence interval is highly desirable. Furthermore, the exact confidence interval can also be used to determine the significance of the coherence estimation.

The independence threshold has been widely used for testing the statistical significance of the coherence estimates. Coherence estimates below this threshold suggest that the two processes are independent (Brillinger, 1975; Carter, 1987; Halliday et al., 1995; Zaveri et al., 1999). However, people are generally more interested in coherence estimates above this threshold. For a coherence value much higher than the threshold of independence, the two signals are highly unlikely to be independent. Thus, it is reasonable to assume that two signals are correlated. However, it does not directly prove the existence of correlation. Therefore, when the coherence values are above but close to the threshold, due to weak correlation or inefficient estimation, e.g. due to limited number of windows, the statistical significance in coherence estimates will be in doubt. To overcome this problem, two supplementary statistical tests are proposed to test the significance of the coherence estimates. One is the probability of detection, i.e. while a threshold E_I is used to test the hypothesis that MSC equals 0 with a probability of P_I, the estimates of coherence above this threshold can be seen as the evidence of linear association between two processes at certain probability P_D (Carter, 1987). If P_D is larger than a significant probability, such as 0.95, there is true correlation between two processes. When the estimates of coherence are above the independence threshold, but their probabilities of detection do not reach the significance level, it suggests that the two signals are not statistically independent, but the significant linear association between them is not sufficiently confirmed. It is also noticed that when the estimated coherence is actually very small, and close to the independence threshold, the difference between the true and estimated probability of detection increases. In this case, it is necessary to adjust the parameter of the probability of detection. If the coherence value is larger than the independence threshold and the true probability of detection is larger than 0.95, the difference between the true and estimated probability of detection is approximately constant and irrelevant to the coherence value and the number of data segments (Table 1). We would recommend 0.97 as a more reliable significant level than 0.95 for the estimated probability of detection particularly when

the coherence value is small and close to the independent threshold.

In order to measure the significance of the coherence estimates, another statistical test based on the exact confidence interval of the coherence estimates is proposed. The hypothesis (H_0) is: MSC > 0 against H_1: MSC $= 0$ at a frequency is tested by the comparison of the confidence intervals. If the lower bound of the one side confidence interval with confidence coefficient 0.95 is larger than the independence threshold E_I, H_0 is accepted with $\alpha < 0.05$ and the MSC is significantly larger than 0. By increasing values of n_d steeper probability of detection curves and narrow confidence band are obtained. The statistical tests are more powerful to detect the significance of the estimates.

To investigate the functional correlation between the symptom-related EMGs and brain FPs presents a very good case for using coherence estimation. However, given the features of the symptom-related FPs, the coherence estimation needs to be optimised and extra statistical tests may be necessary. In the case presented in the current report, increasing the value of n_d from 10 to 75 results in a clear change in the value and frequency resolution of the MSC estimates with narrower confidence interval and higher detection probability at the tremor frequency. The significant coherence is also detected at the double tremor frequency with 75 windows but not with 10 windows (Fig. 5). The significant coherence is concealed due to the larger bias error and random error caused by the fewer windows.

One important issue which needs to be addressed here is the influence of stationarity or non-stationarity of the signals on the coherence estimation. Generally speaking the MSC estimator is most suitable for analysing the time-series which have a zero-mean and wide-sense stationarity with a constant variance over time. The trend of the time-series will cause over-rejection of the null hypotheses in regressions of one signal on another, leading to false positive relationships (Yaffee and McGee, 2000). Also if the variance of the data segments are not stable, the estimated coherence will be dominated by the subset of segments with the largest variance. The statistical tests on the coherence estimates may then be misinterpreted. The stationarity of signals may be evaluated using the run or side tests for the sequence of mean values and standard deviations from the data segments (Kittel, 1977; Manuca and Savit, 1996; Sugimoto et al., 1977). One method to exclude the influence of the non-stationarity was suggested by removing the mean value and normalising standard deviation across the data segments in pooled coherence estimation (Baker, 2000; Halliday et al., 1999).

Stationarity of the neural signals usually relates to the state or specific physiological/pathological condition over which the signal is recorded. Most of the neural signals exhibit non-stationary activity to some extent. In practice, the influence of non-stationarity on coherence estimation may be limited by controlling the recording condition and selecting the data segments over which the signal is stationary. In practice, there is always a trade-off between the bias and random error of the estimator induced by a limited number of data segments and the influence of non-stationarity with a large number of segments. This trade-off is easier to determine when the coherence estimates are large in comparison to when they are small. Undoubtedly further work is needed to find indices for determining the optimal data length based on stationarity of the signals. In the present report, we estimated coherence between the tremor-related LFPs and EMG over a length of 150 s to illustrate the influence of the segment number on efficacy of an estimator and accuracy of the statistical tests. The signals were recorded while the patient was fully resting and the tremor activity was persistent without obvious intermittency. The LFP signal was stationary with constant mean and variance, while the rectified EMG showed a smooth decline in the standard deviations over segments, but no sudden changes. Given the facts that the coherence estimates at frequencies of 4.8 and 9.7 Hz were much higher than the independence threshold and satisfied all three statistical tests, we concluded that the LFPs and EMGs were significantly coherent at the tremor and the double-tremor frequencies.

In summary, we have proposed practical algorithms for optimising a coherence estimator and generating supplementary statistical tests, and demonstrated the utility of the above measures in assessing the functional correlation between the tremor-related oscillatory STN FPs and the surface EMG of the contralateral forearm extensor in Parkinsonian patients.

Acknowledgements

Thanks to Mr. Jonathan Winter for his technical support and to Mrs. Carole Joint for helping with patient care. This work is supported by research grants from the Medical Research Council and the Wellcome Trust, UK.

References

Baker SN. Pooled coherence can overestimate the significance of coupling in the presence of inter-experiment variability. J Neurosci Methods 2000;96:171–2.

Bendat JS, Piersol AG. Engineering applications of correlation and spectral analysis. 2nd ed. New York: Wiley; 1993.

Bendat J, Piersol A. Random data: analysis and measurement procedures. 3rd ed. New York: Wiley; 2000.

Brillinger D. Time series: data analysis and theory. New York: Holt, Rinehart and Winston; 1975.

Brown P, Farmer SF, Halliday DM, Marsden J, Rosenberg JR. Coherent cortical and muscle discharge in cortical myoclonus. Brain 1999;122:461–72.

Carter GC. Receiver operating characteristics for a linearly thresholded coherence estimation detector. IEEE Trans Acoust Speech, Signal Process 1977;ASSP-25:90–2.

Carter GC. Coherence and time delay estimation. Proc IEEE 1987;75: 236–55.

Carter GC, Nuttall AH, Knapp CH. Statistics of the estimate of the magnitude-coherence function. IEEE Trans Audio Electroacoust 1973;AU-21:388–9.

Clausen A, Cochran D. Asymptotic analysis of the generalized coherence estimate. IEEE Trans SP 2001;49:45–53.

Halliday DM, Rosenberg JR, Amjad AM, Breeze P, Conway BA, Farmer SF. A framework for the analysis of mixed time series/point process data-theory and application to the study of physiological tremor. Prog Biophys Mol Biol 1995;64:237–78.

Halliday DM, Conway BA, Farmer SF, Rosenberg JR. Load-independent contributions from motor-unit synchronization to human physiological tremor. J Neurophysiol 1999;82:664–75.

Kay S. Modern spectral estimation. New Jersey: Prentice Hall PTR; 1987.

Kittel P. A test for stationary random process. Phys Lett A 1977;60A: 281–2.

Liu X, Rowe J, Nandi D, Hayward G, Parkin S, Stein J, et al. Localisation of the subthalamic nucleus using radionics image fusion(TM) and stereoplan(TM) combined with field potential recording: a technical note. Stereotact Funct Neurosurg 2001;76:63–73.

Liu X, Ford-Dunn H, Hayward G, Nandi D, Miall C, Aziz T, et al. The oscillatory activity in the Parkinsonian subthalamic nucleus investigated using the macroelectrodes for deep brain stimulation. Clin Neurophysiol 2002a;113:1667–72.

Liu X, Griffin IC, Parkin SG, Miall RC, Rowe JG, Gregory RP, et al. Involvement of the medial pallidum in focal myoclonic dystonia: a clinical and neurophysiological case study. Mov Disord 2002b;17: 346–53.

Manuca R, Savit R. Stationarity and nonstationarity in time series analysis. Physica D 1996;99:134–61.

Marsden JF, Ashby P, Limousin Dowsey P, Rothwell JC, Brown P. Coherence between cerebellar thalamus, cortex and muscle in man: cerebellar thalamus interactions. Brain 2000;123:1459–70.

Scannell EH, Carter GC. Confidence bounds for magnitude-squared coherence estimates. IEEE Trans Acoust Speech, Signal Process 1978;ASSP-26:475–7.

Stuart A, Ord J, Arnold S, Kendall M. Kendall's advanced theory of statistics: classical inference and the linear model. 6th ed. London: Edward Arnold; 1999. p. 116–64.

Stuart A, Keit Ord J, Arnold S. Kendall's advanced theory of statistics: classical inference and the linear model. 6th ed. Oxford University Press; 2001. p. 116–64.

Sugimoto H, Ishii N, Iwata A, Suzumura N. Stationarity and normality test for biomedical data. Comput Programs Biomed 1977;7:293–304.

Wang SY, Tang MX. Exact confidence interval for magnitude-squared coherence estimates. IEEE Signal Process Lett 2004;11:1–4.

Yaffee R, McGee M. Introduction to time series analysis and forecasting. Boston: Academic; 2000. p. 6–7.

Zaveri HP, Williams WJ, Sackellares JC, Beydoun A, Duckrow RB, Spencer SS. Measuring the coherence of intracranial electroencephalograms. Clin Neurophysiol 1999;110:1717–25.